外层氧气引入对 GPCA-TIG 焊焊缝性能的影响

黄 勇[1]， 郭 卫[1]， 王艳磊[2]

(1. 兰州理工大学 省部共建有色金属先进加工与再利用国家重点实验室，兰州 730050；
2. 海芙德建筑产品(上海)有限公司，上海 201601)

摘 要： 针对 SUS304 不锈钢，采用传统 TIG 焊和 GPCA-TIG 焊进行工件表面熔焊，对外层气体引入氧气的 GPCA-TIG 焊和传统 TIG 焊焊缝的氧含量、显微组织、拉伸性能和低温冲击韧性进行了测定. 结果表明，GPCA-TIG 焊焊缝组织主要为奥氏体和铁素体，铁素体形态以骨架状和板条状为主. 外层引入氧气时，焊缝中的氧含量增加，耦合度为 +2 时焊缝中的氧含量高于耦合度为 0 时的，焊缝的抗拉强度均略低于母材的. 耦合度为 0 的 GPCA-TIG 焊焊缝冲击性能与传统 TIG 焊的相同，耦合度为 +2 的焊缝低温冲击韧性有所降低，达到传统 TIG 焊的 85%.

关键词： GPCA-TIG 焊； O 元素含量； 耦合度； 拉伸性能； 低温冲击韧性
中图分类号： TG 406 **文献标识码：** A **文章编号：** 0253 - 360X(2016)09 - 0005 - 04

0 序 言

从 20 世纪 60 年代巴顿焊接研究所提出活性焊接技术以来[1]，该方法引起了世界范围内的广泛关注. 经过不断深入而系统的研究，兰州理工大学黄勇[2,3]提出了一种新型的活性焊接方法——气体熔池耦合活性 TIG 焊(GPCA-TIG 焊，gas pool coupled activating TIG welding). 与以往的活性焊接方法相比，该方法不需要开发专用的活性剂材料；焊接时不需要增加额外的活性剂涂敷工序和其它辅助工序，操作简易，并可实现焊接过程的全自动化，保证焊接过程稳定；通过调节焊枪内外喷嘴的相对位置微量调节活性气体的引入量与引入区域，实现对焊缝成形与焊缝性能的控制，突显了活性焊接方法低成本、高效率及高质量的特点.

对于铁合金，O 为活性元素，可强烈降低液态金属表面张力，改变熔池表面 Marangoni 对流的流动方向[4]，促使电弧输入热量向熔池底部传输，导致熔深显著增加. 焊缝中 O 元素含量的多少对其性能有着重要的影响，尤其是低温冲击韧性. Sato 等人[5]认为当焊缝中 O 元素含量低于 0.002 0% 或在 0.4% ~ 0.5% 之间时焊缝冲击韧性较高. Terashima 等人[6]发现当 GMAW 焊缝中 O 元素含量低于 0.02% 时，能够提高中低强度钢的冲击韧性，而对于高强钢则冲击韧性降低. 樊丁等人[7]在进行分离电弧 AA-TIG 焊时，发现当辅助电弧活性混合气体中氧气的流量超过 2 L/min 时，焊缝的低温冲击韧性降低较多.

文中对外层气体引入氧气时，不同耦合度下 GPCA-TIG 焊焊缝中的氧含量、焊缝显微组织和力学性能进行分析，并与传统 TIG 焊缝进行比较，综合研究了外层气体引入氧气对 GPCA-TIG 焊焊缝的影响规律.

1 试验方法

试验母材为 SUS304 不锈钢，分别采用传统 TIG 焊和 GPCA-TIG 焊进行工件表面熔焊. GPCA-TIG 焊方法如图 1 所示，内层气体采用纯氩气，外层气体氧气，焊接参数如表 1 所示. 焊前用酒精擦拭工件去

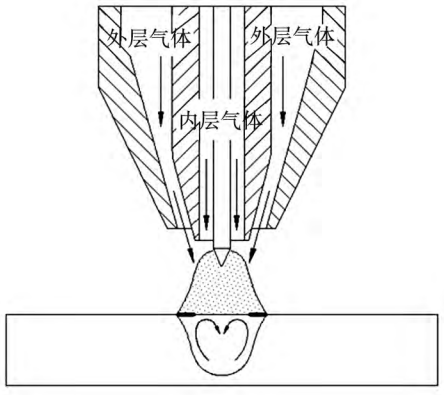

图 1 GPCA-TIG 焊接方法示意图
Fig. 1 Schematic diagram of GPCA-TIG welding method

收稿日期：2015 - 05 - 07
基金项目：国家自然科学基金资助项目(51265029)

除表面油污，然后用砂纸打磨，直到露出金属光泽. 焊后沿垂直焊缝方向截取焊缝金属试样，然后研磨、抛光、腐蚀，观察焊缝金相组织. 采用氮氧分析仪测定焊缝中氧的含量，用扫描电镜对焊缝进行组织观察，并分别进行拉伸试验和 -40 ℃低温冲击试验，通过对比研究氧引入对焊缝的影响规律.

由于外层气体与熔池表面的耦合程度不易直接测量，用焊枪内外喷嘴的相对高度来表征. 当外喷嘴相对于内喷嘴平齐及高 2 mm 时，定义其耦合度 h 分别为 0 和 +2.

表1 GPCA-TIG 焊工艺参数

Table 1 GPCA-TIG welding specifications

焊接电流 I/A	焊接速度 v/(mm·min^{-1})	钨极直径 d/mm	钨极伸出长度 L_1/mm	钨极尖端角度 θ/(°)	电弧长度 L_2/mm	内层氩气流量 Q_1/(L·min^{-1})	外层气体流量 Q_2/(L·min^{-1})	耦合度 h
180	60	2.4	3	45	4	10	5	0 或 +2

2 试验结果

2.1 焊缝成形

由图 2 可知，传统 TIG 焊焊缝熔深较浅，而外层引入氧气的 GPCA-TIG 焊对 8 mm 厚焊材可不开坡口一次性焊透，其焊缝熔宽较窄，表面有轻微氧化，焊缝成形良好. 当耦合度为由 0 变为 +2 时，焊缝背部熔宽变大，熔透能力增强.

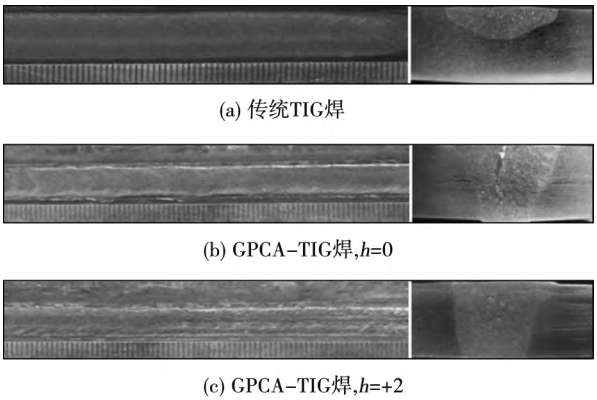

(a) 传统TIG焊

(b) GPCA-TIG焊，h=0

(c) GPCA-TIG焊，h=+2

图2 TIG 焊与 GPCA-TIG 焊的焊缝成形

Fig. 2 Weld shapes of TIG welding and GPCA-TIG welding

2.2 焊缝中氧含量测定

依据国家标准 GB/T11261—2006《钢铁、氧含量的测定、脉冲加热惰气熔融-红外线吸收法》，利用氮氧分析仪对不同耦合度下的 GPCA-TIG 焊缝中的 O 元素含量进行测定，结果如表 2 所示. GPCA-TIG 焊由于外层气体中氧的引入使得焊缝金属中的氧含量高于传统 TIG 焊的，并且随着耦合度增加，氧含量也有微量增加，两者相差 0.000 8%. 由此可知，通过调节焊枪内外喷嘴的相对位置，即调节耦合度 h 可以实现对 GPCA-TIG 焊缝中 O 元素含量的微量控制. 当耦合度增加时，焊枪内外喷嘴的间隙减小，外层保护气体流速增加，气体挺度增加将使更多的外层活性气体进入到电弧和熔池的中心区域，从而使得进入熔池中的氧含量增加.

表2 焊缝中 O 元素含量测试结果

Table 2 Test results of weld oxygen element content

编号	样品名称	耦合度 h	O 元素含量 w(%)
1	TIG 焊	-	0.001 7
2	GPCA-TIG 焊	0	0.009 2
3	GPCA-TIG 焊	+2	0.010 0

2.3 焊缝组织

分别对传统 TIG 焊和外层引入氧气的 GPCA-TIG 焊焊缝显微组织进行观察. 如图 3 所示，全部焊缝的熔合区和焊缝区组织都由奥氏体和铁素体两相组成，且铁素体都为板条状和骨架状两种，如图 4 所示. 组织形态从熔合区到焊缝中心区由柱状晶变为等轴晶. 在焊缝中心区域，传统 TIG 焊全为细小的等轴晶，而两种耦合度下的 GPCA-TIG 焊都还有一部分柱状晶. 相对于传统 TIG 焊，GPCA-TIG 焊焊缝中晶粒略有粗化，组织中板条状铁素体较少. 当耦合度从 0 变为 +2 时，焊缝晶粒变得细小，板条状铁素体含量增多.

对焊缝中的铁素体进行 EDS 成分分析，结果如表 3 所示. 板条状铁素体中的铬含量高于骨架状铁素体的，而镍含量比骨架状铁素体的低. 这是因为，SUS304 不锈钢焊缝的凝固方式是 FA 模式，奥氏体是依靠不断消耗铁素体而形成的. 随着相变过程的进行，在残留铁素体中的铬和钼等铁素体生成元素不断富集，而镍、碳、氮等奥氏体元素不断贫化. 随着温度逐渐降低，扩散距离逐渐减小，元素的扩散行为将受到限制，铁素体以紧密排列的板条状形态进行就更为有效. 结果使得铁素体成为横切过原始的枝状晶或胞状晶生长方向的板条形状，且其中的铁

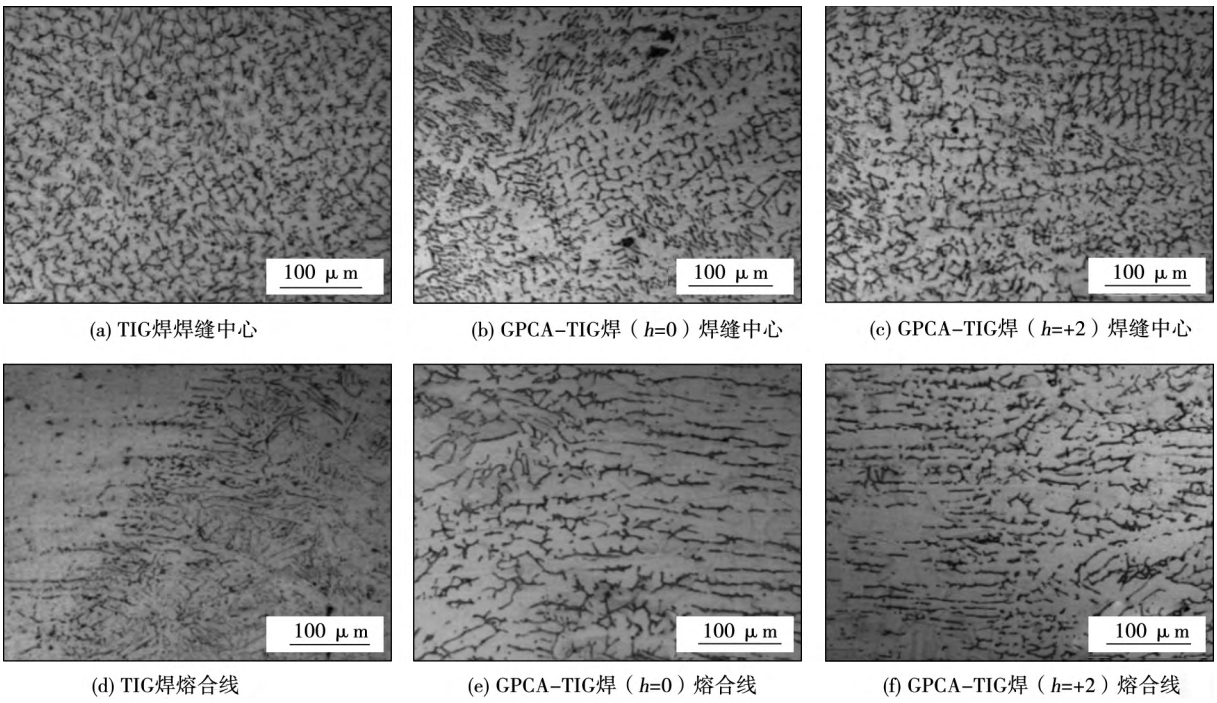

(a) TIG焊焊缝中心　(b) GPCA-TIG焊（h=0）焊缝中心　(c) GPCA-TIG焊（h=+2）焊缝中心

(d) TIG焊熔合线　(e) GPCA-TIG焊（h=0）熔合线　(f) GPCA-TIG焊（h=+2）熔合线

图 3　TIG 焊与 GPCA-TIG 焊焊缝显微组织

Fig. 3　Weld microstructures of TIG welding and GPCA-TIG welding

素体形成元素 Cr 较高，而奥氏体形成元素 Ni 较低.

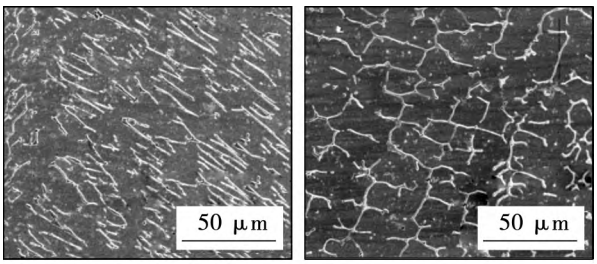

(a) 板条状铁素体　（b）骨架状铁素体

图 4　SEM 下典型焊缝组织形貌

Fig. 4　Typical microstructure morphology under SEM

表 3　铁素体中主要元素化学成分（质量分数，%）

Table 3　Main element contents of ferrite

铁素体类别	Fe	Cr	Ni
板条状	68.6	20.7	6.0
骨架状	68.9	18.1	7.3

2.4　焊缝力学性能

依据国家标准 GB/T228—2002《金属材料室温拉伸试验方法》分别对母材、传统 TIG 焊与 GPCA-TIG 焊焊缝进行拉伸试验，试样尺寸如图 5 所示. 结果如表 4 所示，GPCA-TIG 焊焊缝的强度均略低于母材和传统 TIG 焊焊缝的. 对于 GPCA-TIG 焊，耦合度为 +2 时的焊缝强度要高于耦合度为 0 时的.

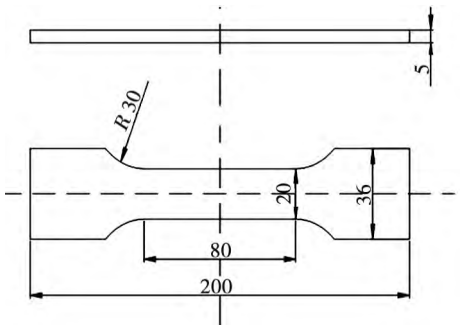

图 5　拉伸试样尺寸（mm）

Fig. 5　Tension specimen size

表 4　焊缝拉伸试验结果

Table 4　Results of weld tensile test

编号	样品名称	耦合度 h	屈服强度 R_{eL}/MPa	抗拉强度 R_m/MPa
1	母材	–	475	775
2	TIG 焊	–	464	742
3	GPCA-TIG + O_2	0	447.5	754
4	GPCA-TIG + O_2	+2	456	764.5

依据国家标准 GB/T229—2007《金属材料夏比摆锤冲击试验方法》分别对传统 TIG 与 GPCA-TIG 焊进行 −40 ℃低温冲击试验，试样的尺寸为 55 mm ×10 mm ×2.5 mm. 结果如表 5 所示，与传统 TIG 焊相比，耦合度为 +2 的 GPCA-TIG 焊焊缝低温冲击韧性有所降低，达到传统 TIG 焊的 85%，而耦合

度为 0 时的则与传统 TIG 焊的相同.

表 5 焊缝冲击试验结果

Table 5 Test results of weld impact

编号	样品名称	耦合度 h	温度 T/℃	冲击吸收功 A_{KV}/J
1	TIG 焊	–	–40	36.67
2	GPCA-TIG + O_2	0	–40	36.33
3	GPCA-TIG + O_2	+2	–40	31.33

3 分析与讨论

在进行不锈钢 GPCA-TIG 焊时,外层活性气体氧气在电弧高温和强电磁场作用下将增加熔池中的氧元素含量,如表 2 所示. 而 O 作为活性元素能够改变表面张力温度系数,使得熔池内的高温金属流态改变,从而显著增加焊缝的熔深.

但从表 4 和表 5 可以看出,O 元素的引入将使得焊缝力学性能略有下降. 其原因分析如下: 一方面,按照 Gibbs 热力学定律,使晶界表面张力降低的溶质原子将偏聚在晶界,造成所谓的正吸附. 而晶界偏聚会使晶界结合力降低,改变焊缝金属性能. 另一方面,O 元素的引入会造成合金元素的烧损,这不但使焊缝形核过程中的形核质点数目减少,造成焊缝晶粒粗大,而且还会增加焊缝中氧化物和氮化物等的含量,从而降低焊缝冲击韧性. 另外,O 元素引入还将通过改变焊接温度场和焊缝成分使得焊缝组织中的铁素体形态和含量发生变化,使得裂纹更易扩展,从而冲击韧性下降. 具体机理还需进一步深入研究.

由于 GPCA-TIG 焊中 O 元素只通过电弧和熔池外围进入熔池金属,焊缝中 O 元素含量增加量较少,并可通过调节耦合度等参数进行控制,其对焊缝冲击性能的有害作用较小. 另外,还可考虑在外层气体中引入 O 元素增加焊缝熔深的同时引入其它焊缝性能有益元素,实现高效率高质量焊接.

4 结 论

(1) GPCA-TIG 焊,外层气路引入氧气时,焊缝表面成形良好,与传统 TIG 焊相比,熔深显著增加,8 mm板材可不开坡口一次性焊透.

(2) GPCA-TIG 焊,外层气路引入氧气时,与传统 TIG 焊相比焊缝中氧含量略有增加. 通过调节耦合度 h 可以实现对 GPCA-TIG 焊缝中 O 元素含量的微量控制.

(3) GPCA-TIG 焊与 TIG 焊焊缝组织均为奥氏体和铁素体; 铁素体沿着奥氏体晶界析出,且铁素体形态主要以骨架状和板条状为主. 与 TIG 焊相比 GPCA-TIG 焊焊缝中晶粒略微粗大,组织中板条状铁素体较少. 当耦合度从 0 变为 +2 时,焊缝晶粒变得细小,板条状铁素体含量增多.

(4) 外层引入氧气时,GPCA-TIG 焊焊缝的强度略低于母材. 与传统 TIG 焊相比,耦合度为 +2 的焊缝低温冲击韧性有所降低,达到传统 TIG 焊的 85%,而耦合度为 0 的 GPCA-TIG 焊焊缝冲击性能与传统 TIG 焊的相同.

参考文献:

[1] Gurevich S M, Zamokov V N, Kushirenko N A. Improving the penetration of titanium alloys when they are welded by tungsten arc process [J]. Automatic Welding, 1965, 18(9): 1 – 5.

[2] 黄 勇, 刘瑞琳, 樊 丁, 等. 气体熔池耦合活性 TIG 焊方法 [J]. 焊接学报, 2012, 33(9): 13 – 14.
Huang Yong, Liu Ruilin, Fan Ding, *et al*. Gas pool coupled activating TIG welding method [J]. Transactions of the China Welding Institution, 2012, 33(9): 13 – 14.

[3] 黄 勇, 郝延召, 刘瑞琳. 耦合电弧钨极 GPCA-TIG 焊工艺 [J]. 焊接学报, 2014, 35(3): 19 – 23.
Huang Yong, Hao Yanzhao, Liu Ruilin. Investigation on coupling arc electrode GPCA-TIG welding process [J]. Transactions of the China Welding Institution, 2014, 35(3): 19 – 23.

[4] 陆善平, 董文超, 李殿中, 等. 不锈钢材料的高效率焊接新工艺 [J]. 金属学报, 2010, 4(11): 1347 – 1364.
Lu Shanping, Dong Wenchao, Li Dianzhong, *et al*. High efficiency welding process for stainless steel materials [J]. Acta Metallurgica Sinica, 2010, 4(11): 1347 – 1364.

[5] Sato Y, Kuwana T. Mechanical properties of extremely low oxygen steel weld metal [J]. Quarterly Journal of the Japan Welding Society, 1993, 11(1): 113 – 119.

[6] Terashima S, Bhadeshia H K D H. Changes in toughness at low oxygen concentrations in steel weld metal [J]. Science and Technology of Welding and Joining, 2006, 11(5): 509 – 516.

[7] 樊 丁, 刘自刚, 黄 勇, 等. 电弧辅助活性 TIG 焊焊缝组织及性能分析 [J]. 焊接学报, 2014, 35(4): 1 – 5.
Fan Ding, Liu Zigang, Huang Yong, *et al*. Structure and properties of arc assisted activating TIG welding [J]. Transactions of the China Welding Institution, 2014, 35(4): 1 – 5.

作者简介: 黄 勇,男,1972 年出生,博士,教授. 主要从事高效焊接技术研究. 发表论文 70 余篇. Email: hyorhot@lut.cn

通讯作者: 郭 卫,男,硕士研究生. Email: gw901212@163.com

MAIN TOPICS, ABSTRACTS & KEY WORDS

Corrosion failure analysis for heat exchanger JING Hongyang[1,2], SHANG Jin[1,2], XU Lianyong[1,2], HAN Yongdian[1,2] (1. School of Materials Science and Engineering, Tianjin University, Tianjin 300350, China; 2. Tianjin Key Laboratory of Advanced Joining Technology, Tianjin 300350, China). pp 1-4

Abstract: During the process of periodic inspection of the heat exchanger, it can be found obvious gap in the surface, which leading to failure of the heat exchanger. In order to investigate the reasons of the failure and keep such incidents from happening again, Metallographic analysis, SEM and electrochemical corrosion perforation are used for E-715 heat exchanger tube sheet weld failure analysis in order to be familiar with its mechanism. It turns out that the heat exchanger corrosion perforation was caused by the electrochemical corrosion. The electrode potential of base metal is higher than that of welding in the service medium which caused the corrosion of welding and final perforation. Meanwhile, the tube medium is a hydrocarbon with a higher carbon content in which the tube surface performed carburization.

Key words: corrosion perforation; electrochemical corrosion; carburization

Effects of oxygen outer gas on weld properties of gas pool coupled activating TIG welding HUANG Yong[1], GUO Wei[1], WANG Yanlei[2] (1. State Key Laboratory of Advanced Processing and Recycling of Non-ferrous Metals, Lanzhou University of Technology, Lanzhou 730050, China; 2. Hymetal Building Components (Shanghai) Co. Ltd., Shanghai 201601, China). pp 5-8

Abstract: Based on SUS304 stainless steel, bead-on-plate experiments for both ordinary TIG welding and GPCA-TIG welding using O_2 as the outer gas were made to evaluate the oxygen content in the weld, micro-structure, the tensile properties and low temperature impact-toughness of the weld. The results show that, the weld micro-structure of GPCA-TIG welding mainly composites of austenite and ferrite. The morphology of ferrite is lacy and vermicular. Oxygen introduced as the outer gas makes the weld oxygen content increase. When the coupling degree is +2, the weld oxygen content is higher than that of coupling degree 0. The tensile strengths of the weld are all slight lower than those of the parent metal. The low temperature impact-toughness of the weld with coupling degree 0 is almost the same with that of TIG welding, while the low temperature impact-toughness value for coupling degree +2 is decreased and only reaches 85% of traditional TIG welding.

Key words: GPCA-TIG welding; oxygen element content; coupling degree; tensile property; low temperature impact-toughness

Forward synthesis ultrasonic images for testing a planar defect CHI Dazhao, MA Shilin, YU Lianyang, GANG Tie (State Key Laboratory of Advanced Welding and Joining, Harbin Institute of Technology, Harbin 150001, China). pp 9-12

Abstract: In order to solve inverse problem of non-destructive weld defect testing, ultrasonic signal for a planar defect is simulated and the images are forward synthesized. Based on Multi-Gaussian Beams theory, ultrasound propagation behaviors are described. It includes in the probe wedge, wedge-testing piece interface and the testing piece. Based on these, an inspective model is established by employing Kirchhoff approximation theory. A bottom surface broken slot used is fabricated and the artificial planar defect is tested using ultrasonic method. Using the model, ultrasonic A-scan lines are simulated and D-, B-scan foreground images are synthesized. The experimental results show that the simulated dada are in better accordance with the measured ones. Forward synthesis can do help to optimize the testing parameter and solve inverse problem of non-destructive characterization.

Key words: ultrasonic testing; simulation; forward synthesis; planar defect

Effects of Si on microstructures and properties of in situ WC reinforced coating XIAO Yifeng[1,2], LI Xuefeng[1,2], DU Hang[1,2], XU Yanfei[1,2], HE Yuehui[3] (1. School of Mechanical Engineering, Xiangtan University, Xiangtan 411105, China; 2. Key Laboratory of Welding Robot and Application Technology of Hunan Province, Xiangtan University, Xiangtan 411105, China; 3. State Key Laboratory of Powder Metallurgy, Central South University, Changsha 410083, China). pp 13-17

Abstract: Effects of Si on microstructures and properties of WC particles reinforced coating with Si content from 0 to 12.5 wt-% prepared by argon arc cladding were analyzed by optical microscopy, scanning electron microscopy (SEM), X-ray diffractometer (XRD), hardness tester and wear tester. The results show that, when Si content is in range of 0 to 5 wt-%, it can promote the nucleation and growth of the WC and inhibit the growth of Fe_3W_3C. When Si is added to 5 wt-%, the wear resistance of the coating was 58 times than that of Q235 steel, which was corresponding to WC particles distributing uniformly in the coating. However, as the Si content increased up to 7.5 wt-%, the wear resistance was only 13.9 times than that of Q235 steel due to the WC grain size decreasing and obvious aggregation.

Key words: in-situ synthesizing; wear resistance; silicon content; WC particle

Comparison analysis of arc light and laser vision sensing weld pool oscillation characteristic signals GU Yufen, DU Leiming, LI Chunkai, SHI Yu (State Key Laboratory of Advanced Processing and Recycling of Non-ferrous Metals, Lanzhou University of Technology, Lanzhou 730050, China). pp 18-22

Abstract: To study the effects of arc light and laser vision sensing weld pool oscillation signals under different welding condition for pulsed GTAW, the system that can obtain arc light intensity with the data acquisition card and collect the projected images with the CCD camera was built for detecting weld pool oscillation frequency in pulsed GTAW, and the comparative analysis about the sensing effects of two methods was carried out. From the experimental results, the quality of signals obtained by two different detection methods for a stationary weld pool shows